J. Physiol. (1986), **380**, *pp.* 75–92
With 6 text-figures
Printed in Great Britain

ACTIVATION OF THE CONTRACTILE APPARATUS OF SKINNED FIBRES OF FROG BY THE DIVALENT CATIONS BARIUM, CADMIUM AND NICKEL

BY D. G. STEPHENSON* AND R. THIELECZEK

*From the Department of Cell Physiology, Ruhr University, Bochum, F.R.G., and the * Department of Zoology, La Trobe University, Bundoora, Victoria, Australia, 3083*

(*Received 18 July 1985*)

SUMMARY

1. The contractile apparatus of mechanically skinned muscle fibres of frog can be reversibly activated by Ba^{2+} and Cd^{2+}.

2. The maximum force induced by both Ba^{2+} and Cd^{2+} is the same as that induced by Ca^{2+} and Sr^{2+}.

3. The ionic concentrations of the divalent cations required to induce 50 % of the maximum activated force at 1 mM-Mg^{2+}, pH 7·10, 22 °C and 250 mM ionic strength are about 8×10^{-7} M for Ca^{2+}, 5×10^{-6} M for Cd^{2+}, $2{\cdot}6 \times 10^{-5}$ M for Sr^{2+} and 7×10^{-4} M for Ba^{2+}.

4. Exposure of the skinned fibre to relatively low Ni^{2+} concentrations (between 10^{-6} and 10^{-5} M) resulted in a transient force response accompanied by an irreversible change in the ability of the preparation to develop force.

5. The Ba^{2+}- and Cd^{2+}-activation curves are considerably flatter than the corresponding curves for Ca^{2+} and Sr^{2+}.

6. An increase in Mg^{2+} concentration from 1 to 3 mM decreased the sensitivity of the contractile apparatus to Ba^{2+} by a factor of about 1·5 without affecting the maximum force response.

7. The Ca^{2+}-activation curve was modified in the presence of subthreshold concentrations of Ba^{2+} and the results indicate that Ba^{2+} could have both an activating and an inhibitory action on the Ca^{2+}-activated force.

8. A kinetic model which can quantitatively explain the results for activation of contraction by Ba^{2+} and Ca^{2+}, is described.

INTRODUCTION

Little is known about the ability of divalent cations other than Ca^{2+} and Sr^{2+} to activate force development in skeletal muscle. Such information can aid in the characterization of the mechanism of force regulation and also contribute to a better understanding of results from experiments with intact fibres, where Ca^{2+} in the bathing solution is replaced by other divalent cations (see e.g. Heilbrunn & Wiercinski, 1947; Caldwell & Walster, 1963; Fischman & Swan, 1967; Matsumura

& Mashima, 1976; Potreau & Raymond, 1980; Almers & Palade, 1981; Caputo, 1981; Frank & Rohani, 1982).

In this study we have used Ba^{2+} and Cd^{2+} either alone or in conjunction with Ca^{2+}, in order to determine the relationship between the isometric force response of mechanically skinned muscle fibres and the ionized concentration of these divalent ions. Furthermore, we have investigated the effect of Ni^{2+} on the activation of the contractile apparatus.

The results show that there are important differences between the modes of force activation by Ca^{2+} and Sr^{2+} on the one hand and by Ba^{2+} and Cd^{2+} on the other hand. Surprisingly (Fischman & Swan, 1967), Ni^{2+} was also found to elicit force in the skinned fibre preparations at concentrations as low as 10^{-6}–10^{-5} M, but the functioning of the contractile apparatus was irreversibly impaired following exposure to Ni^{2+}.

METHODS

Isolation and preparation of fibres

Single twitch fibres from the iliofibularis muscles of healthy frogs (*Rana esculenta*) were dissected and skinned under pharmaceutically pure cold paraffin oil (Merck) using standard techniques employed in our laboratories (Ashley & Moisescu, 1977; Moisescu & Thieleczek, 1978). The skinned fibres were split carefully into thin myofibrillar bundles of 30–80 μm in diameter which were used for the experiments.

Experimental apparatus and general procedure

The mechanical arrangements for attaching the preparation to the force transducer, measuring the fibre geometry and sarcomere length, activation of the preparation and recording force were similar to those previously described (Moisescu & Thieleczek, 1978). After skinning in paraffin oil, the preparation was mounted in the force recording apparatus and then it was transferred for 30 s into the relaxing solution of type B (Table 1) containing, in addition, 0·1 % v/v of the non-ionic detergent Triton X-100. This procedure completely removed the remaining paraffin oil from the fibre surface. Afterwards the preparations were transferred into the relaxing solution B, without Triton, for microscopic measurement of fibre diameter and length as previously described (Moisescu & Thieleczek, 1978). The average sarcomere length in the preparations at rest was between 2·4 and 2·7 μm. The chamber containing the solutions and the methods of changing solutions and controlling the temperature of the solutions are described in detail elsewhere (Moisescu & Thieleczek, 1978). Unless otherwise indicated, each preparation was challenged by complete contraction–relaxation cycles during each experimental run. The preparations were discarded when the maximum force of the second successive control maximum contraction dropped by more than 10 %. The values of the interpolated control contractions were used for normalizing the measured force responses in a way similar to that of Julian (1971).

Solutions

The bathing solutions were prepared using the basic procedures employed in our laboratories (Ashley & Moisescu, 1977; Moisescu & Thieleczek, 1978, 1979; Stephenson & Williams, 1980, 1981, 1982) and the composition of the solutions is indicated in Table 1. In Table 2 are listed the values for the apparent affinity constants which were required for this study. These values were either determined by us for our conditions using potentiometric methods similar to those described earlier (Moisescu & Thieleczek, 1978, 1979; Stephenson & Williams, 1981; Thieleczek, 1982), or were calculated according to Sillén & Martell (1964, 1970). Unless otherwise indicated, the experiments were carried out at room temperature (21–23 °C).

Activation solutions of various concentrations for Ca^{2+}, Sr^{2+} and Ba^{2+} were obtained by mixing corresponding solutions of type CaA, SrA, BaA with solutions of type B. The resulting solutions of type CaA/B and SrA/B covered the whole range of Ca^{2+} and Sr^{2+} concentrations needed to construct a complete steady-state activation curve (Moisescu & Thieleczek, 1979). Mixtures of type

BaA/B provide well buffered Ba^{2+}-activation solutions up to Ba^{2+} concentrations of 0·7 mM. Ba^{2+}-activation solutions of higher free Ba^{2+} concentrations were obtained either by mixing solutions of type BaC with those of type B and adequately adding $MgCl_2$ or by adding appropriate amounts of $BaCl_2$ and $MgCl_2$ to solutions of type BaC or BaD. In the latter case, the solutions had

TABLE 1. Composition of solutions

Soln.	K^+ (mM)	Mg_{total} (mM)	CK (u/ml)	HDTA (mM)	EGTA (mM)	CaEGTA (mM)	SrEGTA (mM)	BaEGTA (mM)	K_2SUC (mM)	Mg^{2+} (mM)	Temp. (°C)
CaA	137	8·05	15	—	—	50	—	—	—	1	10/23
SrA	137	8·5	15	—	10	—	40	—	—	1	23
BaA	137	8·05	15	—	5	—	—	45	—	1	23
BaA*	137	8·05	15	—	—	—	—	50	—	1	10/23
B	137	10·25	15	—	50	—	—	—	—	1	23
B*	137	9·7	15	—	50	—	—	—	—	1	10
H	137	8·45	15	50	—	—	—	—	—	1	10/23
BaC	137	—	15	—	—	—	—	50	—	—	23
BaD	137	—	15	50	—	—	—	—	—	—	23
S	137	—	—	—	—	—	—	—	50	—	23
NiA	237	—	15	30	20	—	—	—	—	—	23

All solutions contained (mM): Na^+, 36; TES, 60; ATP, 8; creatine phosphate, 10; caffeine, 10. The pH of all solutions was adjusted to $7{\cdot}10 \pm 0{\cdot}1$ at the given temperature. The ionic strength was calculated according to the formula $I = 1/2 \sum c_i . z_i^2$, where c_i and z_i represent the concentration and charge of the ionic species i, respectively. I was about 250 mM in all solutions unless otherwise mentioned in the text.

Abbreviations: HDTA, hexamethylenediamine-*N*,*N*,*N*′,*N*′-tetraacetic acid; EGTA, ethyleneglycol-bis-(β-aminoethylether)*N*,*N*′-tetraacetic acid; TES, 2-(2-hydroxy-1,1-bis(hydroxymethyl) ethyl) aminoethane sulphonic acid; ATP, adenosine 5′-trisphosphate; CK, creatine phosphokinase; SUC, succinate.

a slightly increased ionic strength (I, up to 285 mM) and Cl^- concentration (up to 40 mM) compared with the normal activation solutions (I = 250 mM, Cl^- concentration = 20 mM), because the Ba^{2+} levels were higher. A BaATP precipitate appeared in the solutions at free Ba^{2+} concentrations corresponding to more than 90% of the maximum isometric tension. The precipitate acted as an additional Ba^{2+}-buffering system in these solutions. The concentrations of ionized Ba in these solutions could be quantitatively calculated and controlled by using the apparent solubility product of BaATP for our experimental conditions: $L_{app} = 2{\cdot}84 \times 10^{-6}$ M². This constant was estimated by a relatively simple titrimetric method described in detail by Thieleczek (1982). Ca^{2+}-activation solutions of various Ca^{2+} concentrations and of a constant free Ba^{2+} concentration of 5×10^{-5} M were prepared by mixing three types of solutions CaA, BaA* and B* (Table 1) as previously described (Stephenson & Williams, 1980).

Cd^{2+}-activation solutions of differing free Cd^{2+} concentrations were prepared by adding appropriate amounts of $CdCl_2$ and $MgCl_2$ to solutions of type S which contained succinate instead of EGTA. Succinate is a better Cd^{2+}-buffer than EGTA for our conditions. No creatine kinase was added to this type of solution because even low Cd^{2+} concentrations caused denaturation of the enzyme. Corresponding Ca^{2+}-activation solutions of type S contained $CaCl_2$ instead of $CdCl_2$. The problem of Ca contamination in the relatively poorly Ca^{2+}-buffered succinate solutions of type S was overcome partly by making use of a Dowex A1 (Chelex-100) ion exchange column for the preparation of the stock solutions, as described by Blinks, Mattingly, Jewell, van Leeuwen, Harrer & Allen (1978). Atomic absorption spectrophotometric measurements of the Ca concentration of the solutions of type S indicated that the contaminant free Ca^{2+} concentration in the Cd^{2+}-activation solutions was smaller than $2{\cdot}3 \times 10^{-7}$ M for free Cd^{2+} concentrations of less than $3{\cdot}2 \times 10^{-5}$ M.

Ni^{2+}-activation solutions of differing free Ni^{2+} concentrations were prepared by adding suitable amounts of $NiCl_2$ and $MgCl_2$ to solutions of type NiA. The other solutions used in the Ni^{2+}-activation experiments were adjusted to the elevated K^+ concentration of the solution of type NiA (see also Results).

TABLE 2. Apparent affinity constants, K_L^{app}, of the ligands in the bathing solutions for Mg^{2+}, Ca^{2+}, Ba^{2+}, Cd^{2+} and Ni^{2+}

			Experimental conditions			
Ligand (L)	Cation	K_L^{app} (M^{-1})	K^+ (mM)	Na^+ (mM)	pH	Temp. (°C)
EGTA	Mg^{2+}	35 ± 5	100–200	36	7·10	10*
		46 ± 6	100–200	36	7·10	23*
	Ca^{2+}	$(5 \pm 0{\cdot}5) \times 10^6$	100–200	36	7·10	0–23*
	Sr^{2+}	$(2 \pm 0{\cdot}2) \times 10^4$	100–200	36	7·10	0–23*
	Ba^{2+}	$(1{\cdot}18 \pm 0{\cdot}2) \times 10^4$	100–200	36	7·10	0–23*
	Cd^{2+}	$(3{\cdot}1 \pm 0{\cdot}5) \times 10^{11}$	137	36	7·10	23*
	Ni^{2+}	$9{\cdot}6 \times 10^7$	237	36	7·10	23†
HDTA	Mg^{2+}	$8 \pm 1{\cdot}5$	100–200	36	7·10	0–23*
	Ca^{2+}	$6{\cdot}5 \pm 1$	100–200	36	7·10	0–23*
	Sr^{2+}	Negl.	100–200	36	7·10	0–23*
	Ba^{2+}	3	100–200	36	7·10	0–23*
	Cd^{2+}	$(3 \pm 0{\cdot}5) \times 10^4$	137	36	7·10	23*
	Ni^{2+}	$3{\cdot}8 \times 10^7$	237	36	7·10	23†
ATP	Mg^{2+}	$(6{\cdot}2 \pm 0{\cdot}5) \times 10^3$	137	36	7·10	10*
		$(6{\cdot}5 \pm 0{\cdot}5) \times 10^3$	137	36	7·10	23*
	Ca^{2+}	$(3{\cdot}2 \pm 0{\cdot}2) \times 10^3$	137	36	7·10	10*
		$(3{\cdot}4 \pm 0{\cdot}3) \times 10^3$	137	36	7·10	23*
	Sr^{2+}	$(1{\cdot}4 \pm 0{\cdot}2) \times 10^3$	137	36	7·10	10–23*
	Ba^{2+}	450 ± 50	137	36	7·10	10*
		800 ± 100	137	36	7·10	23*
	Cd^{2+}	$(4 \pm 0{\cdot}5) \times 10^4$	137	36	7·10	23*
	Ni^{2+}	$8{\cdot}3 \times 10^4$	237	36	7·10	23†
Creatine phosphate	Mg^{2+}	$12 \pm 1{\cdot}5$	100–200	36	6·6–7·6	0–23*
	Ca^{2+}	$\leqslant 20$	100–200	36	6·6–7·6	0–23*
	Sr^{2+}	$8 \pm 1{\cdot}5$	100–200	36	7·10	0–23*
	Ba^{2+}	15 ± 1	100–200	36	7·10	0–23*
	Cd^{2+}	50 ± 7	137	36	7·10	23*
Succinate	Mg^{2+}	16	137	36	7·10	23†
	Ca^{2+}	16	137	36	7·10	23†
	Cd^{2+}	124	137	36	7·10	23†

* Apparent affinity constants measured in our laboratories using the potentiometric method of Moisescu & Thieleczek (1979).

† Apparent affinity constants calculated from the data compiled by Sillén & Martell (1964, 1970). The calculated affinity constants for Ni^{2+} correspond to a free Ni^{2+} concentration of 10^{-5} M.

Negl., negligible.

RESULTS

Force activation by Ba^{2+}

EGTA could only be used as an adequate buffer for Ba^{2+} up to concentrations of about 1 mM (Table 2). The maximum isometric force response that could be obtained with the EGTA solutions of type BaA/B was only about 40% of the maximum Ca^{2+}-activated force responses for otherwise similar conditions (Fig. 1*A* and *B*). In order to raise the Ba^{2+} concentration in solutions above 1 mM, new measurements had to be made for the estimation of several stability constants involving Ba^{2+} and

new stock solutions had to be formulated (see Methods). With these solutions (BaC and BaD, Table 2) we increased the free Ba^{2+} concentration up to about 14 mM while maintaining an ionic environment around the preparations similar to that provided by the solutions containing EGTA. As can be seen in Fig. 1*C–F*, the force responses

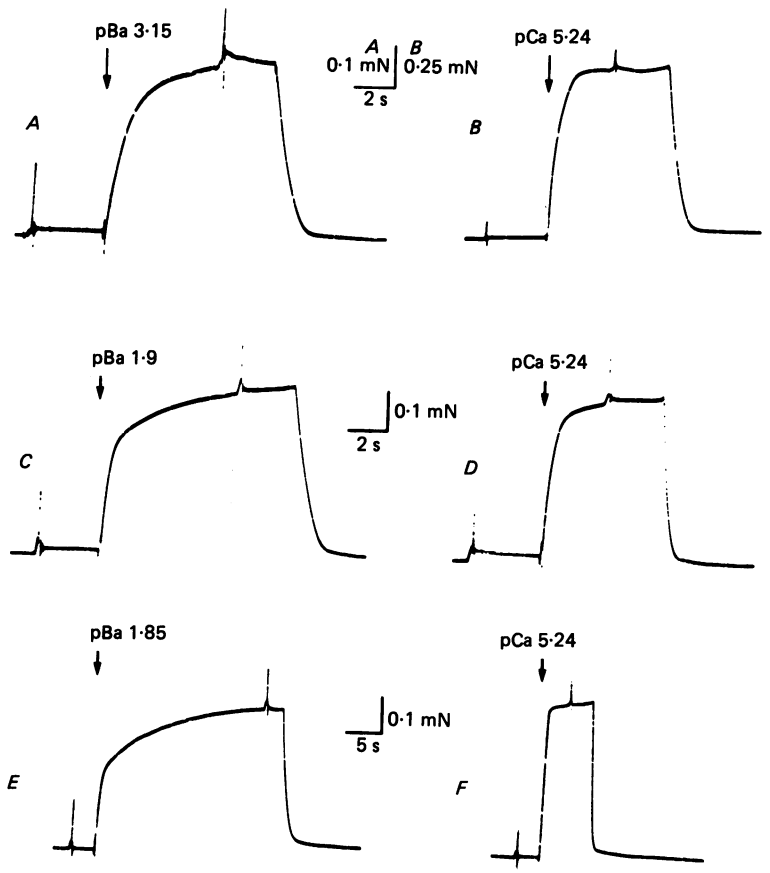

Fig. 1. Maximum Ba^{2+}-induced contractions of three different myofibrillar preparations obtained with different types of Ba^{2+}-activation solutions (*A*, *C* and *E*) and subsequent maximum Ca^{2+} activation of the respective preparations in a solution of type CaA/B with pCa 5·24 (*B*, *D* and *F*) at 1 mM-Mg^{2+}. The preparations were equilibrated for 3 min in a relaxing solution of type H/BaA* with 0·33 mM-EGTA and a subthreshold Ba^{2+} concentration (8×10^{-5} M) before each activation (arrow) in Ba^{2+}-activation solutions of type BaA/B (*A*), BaD (*C*) and BaC (*E*). Before maximum Ca^{2+} activation the fibres were equilibrated for 3 min in a solution of type H/B with 0·1 mM-EGTA. Fibre dimensions (diameter/length): 80 μm/2·2 mm (*A* and *B*), 60 μm/2·1 mm (*C* and *D*) and 50 μm/1·9 mm (*E* and *F*).

induced by 12·6 mM- and 14 mM-Ba^{2+} were almost the same as the maximal Ca^{2+}-activated force response at a pCa of 5·24. The relation between the ionized Ba^{2+} expressed as pBa ($= -\log [Ba^{2+}]$) and relative isometric force for one preparation is shown in Fig. 2*A*, together with representative force–pCa and force–pSr relations. It can be seen that the Ba^{2+}-activation curve is significantly flatter than either the

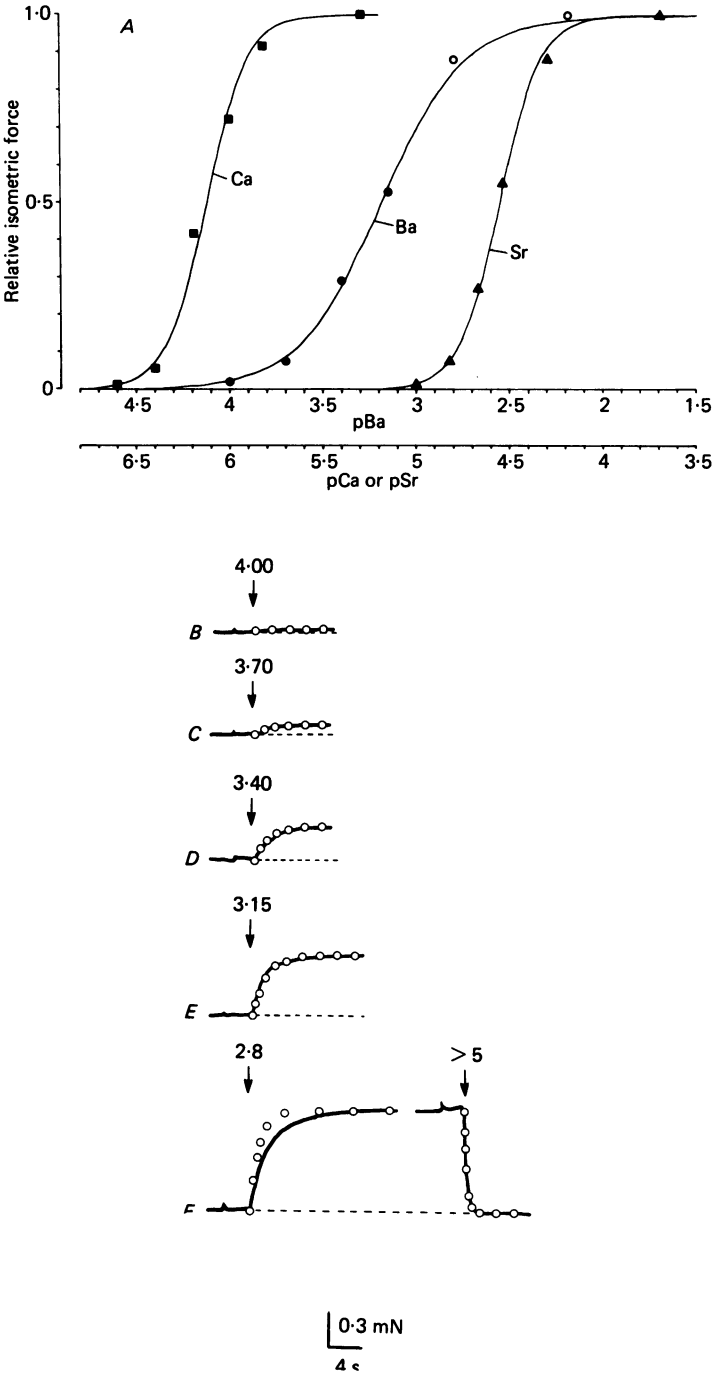

Fig. 2. For legend see opposite.

Ca^{2+}- or the Sr^{2+}-activation curves. This characteristic is reflected in the value of the Hill coefficient associated with the activation curve which is 2 for Ba^{2+} and 4 for Ca^{2+} and Sr^{2+}. From Fig. 2*A* it can also be seen that the sensitivity for Ba^{2+} of the contractile apparatus in frog twitch fibres is significantly lower than that for Ca^{2+} and Sr^{2+}. Thus, if the free concentrations of the three activating ions required to produce 50 % maximum force (Ca_{50}, Sr_{50} and Ba_{50}) are compared, then from Fig. 2*A* the following proportions are obtained: $Ca_{50}:Sr_{50}:Ba_{50} = 1:36:870$.

One should be aware of the decrease in the concentration of $MgATP^{2-}$ in the activating solutions when the concentration of the divalent ions increases. The decrease is, however, generally small (less than 15 %) for conditions where force is near the maximal level, and therefore this should not greatly modify the availability of $MgATP^{2-}$ to the contractile apparatus in the core of the preparations. As an indication of the change in $MgATP^{2-}$ concentration in the activating solutions we have included in the legends of all relevant Figures (Figs. 2–5) the corresponding values of the $MgATP^{2-}$ concentration at 0, 50 and 90 % of maximum activation.

The kinetics of the Ba^{2+}-induced force development were considerably slower (Fig. 2*B–F*) than those for Ca^{2+}, when the concentration of Ba^{2+} was suddenly changed in the preparations by using the set of solutions BaA/B or BaD and the method described previously by Moisescu & Thieleczek (1978, 1979). Theoretical calculations similar to those of Moisescu (1976) and Stephenson & Williams (1981) indicate that the time course of the isometric force response, $P(t)$, following sudden changes in $[Ba^{2+}]$ (both rises and falls) and the steady-state isometric force–pBa relation can be qualitatively explained for $[Ba^{2+}] \leqslant 0{\cdot}7$ mM by the following reaction scheme:

$$Ba^{2+} + R \underset{k'_{-1}}{\overset{k'_1}{\rightleftharpoons}} BaR + Ba^{2+} \underset{k'_{-2}}{\overset{k'_2}{\rightleftharpoons}} Ba_2R \propto P(t), \qquad (1)$$

where R is the regulatory unit of the contractile apparatus and k'_1, k'_{-1}, k'_2 and k'_{-2} are rate constants of reaction. The results obtained with the fibre in Fig. 2*A*

Fig. 2. *A* shows Ba^{2+}-, Ca^{2+}- and Sr^{2+}-activation curves of individual frog myofibrillar preparations at 1 mM-Mg^{2+}. The experimental points were obtained with solutions of type BaA/B (●) and BaD (○) for Ba^{2+}, CaA/B (■) for Ca^{2+} and SrA/B (▲) for Sr^{2+} respectively. The theoretical curves were drawn using a Hill coefficient of 2 for Ba^{2+} and 4 for Ca^{2+} and Sr^{2+} (see text). $MgATP^{2-}$ concentration in solutions was 6·9 mM at 0 force, and 6·9 mM (6·9 mM), 6·9 mM (6·9 mM) and 6·5 mM (5·8 mM) at 50 % (90 %) activation by Ca^{2+}, Sr^{2+} and Ba^{2+} respectively. In *B–F* are individual Ba^{2+}-induced force responses which were used to construct the Ba^{2+}-activation curve given in *A*. Before each activation (arrow) in solutions of type BaA/B (*B–E*) and BaD (*F*) the preparation was equilibrated for 3 min in a relaxing solution of type H/B containing 0·1 mM-EGTA. The pBa values in the activation solutions are indicated above arrows. *F* shows also the time course of relaxation in a solution of type B after 3 min of activation in the weakly Ba^{2+}-buffered solution BaD. The points (○) superimposed on the force records represent the time course of the force transients predicted by the reaction scheme (1) presented in the text. The poorer fit seen in *F* between the observed traces and the predicted results is due to the slow equilibration of the free Ba^{2+} concentration inside the preparation because the activation solution BaD used in this case had weak Ba^{2+} buffering (see Moisescu & Thieleczek, 1978). Fibre dimensions (diameter/length): 80 μm/2·2 mm for Ba^{2+}, 50 μm/1·6 mm for Ca^{2+} and 70 μm/1·9 mm for Sr^{2+}.

(Ba^{2+}-activation curve) and Fig. 2*B–E* could be accurately predicted using eqn. (1) and the following values for the rate constants:

$$k'_1 = 5{\cdot}25 \times 10^2 \text{ M}^{-1} \text{ s}^{-1}; \quad k'_{-1} = 7{\cdot}5 \text{ s}^{-1}; \quad k'_2 = 8{\cdot}05 \times 10^4 \text{ M}^{-1} \text{ s}^{-1}; \quad k'_{-2} = 2{\cdot}3 \text{ s}^{-1}.$$

Force–pBa results obtained with nine different preparations are summarized in Fig. 3*A*. As expected (Moisescu & Thieleczek, 1979), the curve obtained with mean values is even flatter than the individual curves for separate preparations. The Hill coefficient for the curve in Fig. 3*A* is 1·6.

In a different series of experiments we have investigated the effect on the force–pBa activation curves of raising Mg^{2+} concentration from 1 to 3 mM. In these experiments we have used solutions of type BaC/B or BaC and the results obtained with eleven different preparations are shown in Fig. 3*B*. The maximum force response induced by Ba^{2+} was the same in the presence of either 1 or 3 mM-Mg^{2+}, and the curve for 3 mM-Mg^{2+} was shifted by 0·18 logarithmic units towards higher Ba^{2+} concentrations. This shift is consistent with a competitive inhibitory action of Mg^{2+} on the Ba^{2+}-activation process and is similar to the shift reported by Donaldson & Kerrick (1975) for the force–pCa curve with rising Mg^{2+} concentration. The Hill coefficient for both curves (1 and 3 mM-Mg^{2+}) is 1·4. It is important to note that the curve for 1 mM-Mg^{2+} is very similar with respect to its shape and position on the pBa axis to the curve shown in Fig. 3*A* despite the fact that the Ba^{2+}-activation solutions used in the two series of experiments were quite different in composition. This similarity of the results demonstrates that the experimental conditions for these Ba^{2+} experiments were very well controlled.

Compared with the force–pCa curves, the significantly flatter force–pBa curves indicate either a lower degree of co-operativity in the functional regulatory unit between the Ba ions, or a smaller number of Ba ions regulating the functional unit, or both, than is the case with the Ca ions (see eqn. (1) and Moisescu, 1976). In order to find out more about the nature of this difference, we measured force while Ba^{2+} concentration was maintained at a constant subthreshold level, and the level of Ca^{2+} concentration was increased in the solutions. In order to obtain an unequivocal quantitative interpretation of the results, it was critical to obtain Ca^{2+}-activation curves on the same preparation in the presence and absence of Ba^{2+}. This experiment was therefore conducted at 10 °C since we had found from our own experience that the frog skinned muscle preparation deteriorates more slowly at lower temperatures. New solutions were made for experiments conducted at this temperature (Table 1) and we chose a Ba^{2+} concentration of 5×10^{-5} M which was just below the Ba^{2+} threshold for contractile activation in these solutions. This Ba^{2+} concentration was maintained in all solutions, including the relaxing solutions.

The results obtained with two individual myofibrillar preparations are shown in Fig. 4. It is clear that in the presence of Ba^{2+} the force–pCa curve rises less steeply when the ionized Ca concentration increases. The Hill coefficient for this curve is close to 2 and is similar to that for Fig. 2*A* when Ba^{2+} alone was the activating ion. It is also important to note that the Ca^{2+} threshold for force activation in the presence of Ba^{2+} was significantly shifted to higher pCa values (lower Ca^{2+} concentration) compared with the Ca^{2+} threshold in the absence of Ba^{2+}. This result would be expected if Ba^{2+} and Ca^{2+} could replace each other in some steps of the reaction

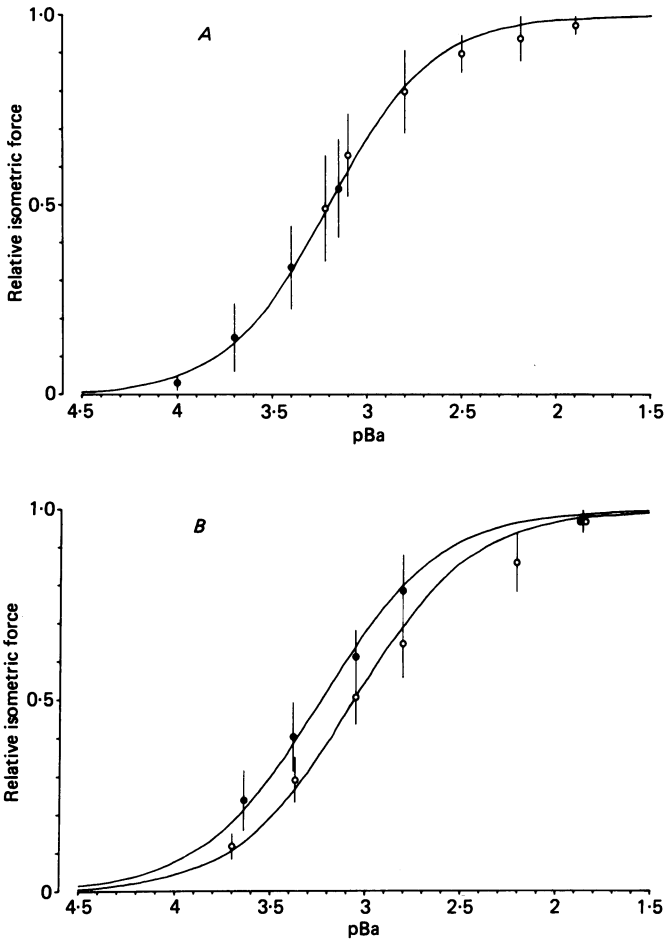

Fig. 3. *A* shows a complete Ba^{2+}-activation curve at 1 mM-Mg^{2+} obtained with Ba^{2+}-activation solutions of type BaA/B (●) and BaD (○). The results (mean value ± S.D.) were obtained with nine different preparations. The continuous curve was drawn using a Hill coefficient of 1·6. In *B* is illustrated the influence of increasing the free Mg^{2+} concentration from 1 mM (●) to 3 mM (○) on the relative force–pBa curve. The results (mean value ± S.D.) were obtained with eleven different preparations. Solutions of type BaC/B were used for pBa $\geqslant$ 3·15 and solutions of type BaC for pBa $<$ 3·15. The continuous curves were drawn using a Hill coefficient of 1·4. $MgATP^{2-}$ concentration in the relaxing solutions was 6·9 mM at 1 mM-Mg^{2+} and 7·6 mM at 3 mM-Mg^{2+}. $MgATP^{2-}$ in the activating solutions at 50% (90%) maximum force was 6·5 mM (5·6 mM) for *A*, 6·5 mM (5·4 mM) for *B* at 1 mM-Mg^{2+}, and 7·3 mM (6·5 mM) for *B* at 3 mM-Mg^{2+}.

leading to force activation. However, force saturates at significantly higher Ca^{2+} concentrations in the presence of Ba^{2+} than in its absence (Fig. 4) indicating that Ba^{2+} compete with Ca^{2+} in some other steps of the reaction which do not lead to force activation when Ba^{2+} is the reacting ion.

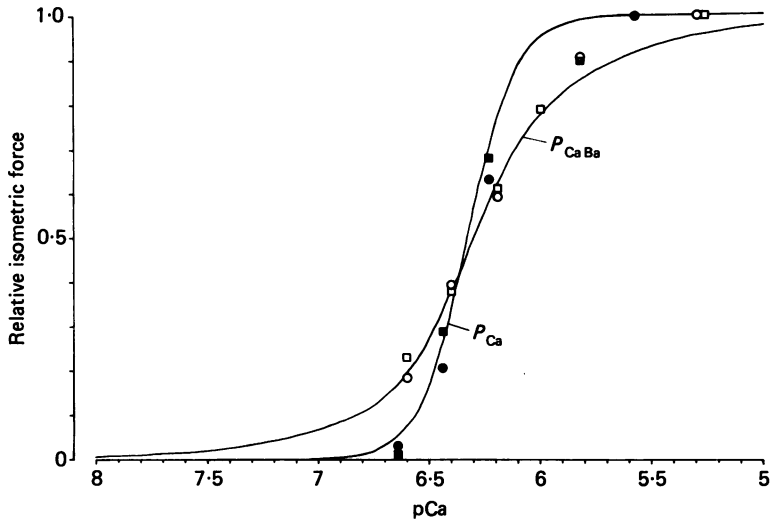

Fig. 4. Ca^{2+}-activation curves of the two individual myofibrillar preparations (○, ● and □, ■) at 1 mM-Mg^{2+} in the presence of 5×10^{-5} M-Ba^{2+} (○, □; P_{CaBa}) and in the absence of Ba^{2+} (●, ■; P_{Ca}). The preparations were equilibrated for 3 min in a relaxing solution of type H/B* = 500/1 before each activation in Ca^{2+}-activation solutions of type CaA/B* (●, ■) and in a relaxing solution of type H/B*/BaA* = 500/1/1·3 before each activation in solutions of type CaA/BaA*/B* (○, □) which contained 5×10^{-5} M-Ba^{2+}. $MgATP^{2-}$ concentration in all solutions corresponding to force levels less than 90% maximum force was within the range 6·85 to 6·95 mM. The theoretical curves P_{Ca} and P_{CaBa} (continuous lines) were derived from eqns. (2)–(6) using the following parameters (see Appendix) $K_1^{Ca} . K_2^{Ca} . K_3^{Ca} . K_4^{Ca} = 2 \times 10^{25}$ M^{-4} for P_{Ca}, and $A = 2 \times 10^{25}$ M^{-4}, $B = 5 \times 10^{18}$ M^{-3} and $C = 7 \times 10^5$ M^{-1} for P_{CaBa}. The dimensions of the preparations were (diameter/sarcomere length/length) 50 μm/2·7 μm/1·9 mm and 50 μm/2·7 μm/2·0 mm for the fibres represented by ○, ● and □, ■, respectively. Temperature 10 °C.

Force activation by Cd^{2+}

The Cd^{2+} concentration in the Cd^{2+}-activation solutions was buffered by 50 mM-$succinate^{2-}$ and 8 mM-ATP (see Table 1, solution S). $EGTA^{2-}$ could not be used as a Cd^{2+} buffer for the concentration range of interest (10^{-7}–10^{-4} M) owing to its very high affinity for Cd^{2+} (Table 2). Cd^{2+} could not be buffered with 50 mM-hexamethylenediamine-*N*,*N*,*N*′,*N*′-tetraacetic acid (HDTA) over the above range because of the formation of a Cd–HDTA complex which precipitates out of solutions. Creatine kinase was also omitted from the Cd^{2+}-activation solutions owing to the formation of a precipitate with Cd^{2+}. All the preparations used in these experiments had a diameter of less than 40 μm to ensure that no significant depletion of ATP took place during activation in the core of the preparations due to the absence of exogenous creatine kinase. The endogenous creatine kinase of myofibrillar origin within the preparations would have further contributed to buffer the ATP within these preparations adequately (Walliman, Turner & Eppenberger, 1977; Saks, Rosenstraukh, Smirnov & Chazov, 1978). Great care was taken to avoid any Ca^{2+} contamination in these Cd^{2+} solutions and to ensure this, all stock solutions used for Cd^{2+} activation were passed through a Chelex-100 ion exchanger to remove Ca^{2+}. Ca^{2+} concentration

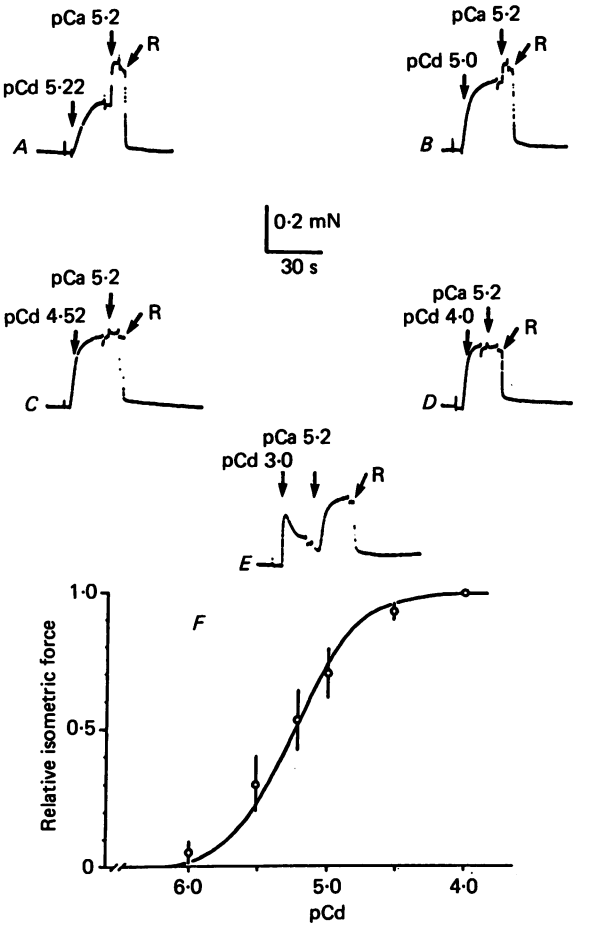

Fig. 5. *A–E* show force responses of thin myofibrillar preparations in Cd^{2+}-activation solutions of type S of different pCd and when maximally activated in a solution of type CaA/B with pCa 5·2. Before each Cd^{2+} activation, the preparations were initially equilibrated for 2 min in a relaxing solution of type S containing 0·02 mM-EGTA and then were incubated in an EGTA-free solution of type S for 60 s. On each trace, R marks the relaxation of a maximally Ca^{2+}-activated fibre in a relaxing solution of type B. $MgATP^{2-}$ concentration in solutions was 6·9 mM at 0 force, 6·7 mM at 50 % force and 6·3 mM at 90 % force. Fibre dimensions (diameter/length): 35 μm/2·3 mm for *A–C* and 40 μm/2·1 mm for *D* and *E*. *F* shows a Cd^{2+}-activation curve at 1 mM-Mg^{2+} obtained using the method demonstrated under *A–D*. The plotted results (mean value $\pm$ absolute scatter) were obtained with fourteen different preparations. The continuous curve was drawn using a Hill coefficient of 1·8.

in these solutions was below 3×10^{-7} M as deduced from atomic absorption spectrophotometric measurements and from the lack of force development in the absence of Cd^{2+}.

Taking the above mentioned precautions, the maximum level of force induced by Cd^{2+} was similar to that induced by Ca^{2+} (Fig. 5*D*). However, the preparations deteriorated rapidly after exposure to Cd^{2+} and it was not possible to obtain a

complete force–pCd (= $-\log [Cd^{2+}]$) curve from one single preparation. Each preparation was activated in a Cd^{2+} solution and was then fully activated by Ca^{2+} (pCa 5·2). The preparation was discarded if the maximal Ca^{2+}-activated force was less than 85% of the initial maximal Ca^{2+}-activated response before exposure to the Cd^{2+} solutions. The Cd^{2+}-activation results obtained with fourteen preparations are shown in Fig. 5*F*. The relative steady-state Cd^{2+}-activated force responses in Fig. 5*F* can be well fitted by a Hill curve with a coefficient of 1·8 which is similar to that for the Ba^{2+}-activated responses (Fig. 3).

An interesting point to note is that the force response declined markedly when the myofibrillar preparations were maximally activated by Cd^{2+} in the presence of a relatively high concentration of $CdATP^{2-}$ compared with $MgATP^{2-}$. Such an example is shown in Fig. 5*E* when the myofibrillar bundle was transferred from a relaxing solution with 6·9 mM-$MgATP^{2-}$ to a Cd^{2+}-activating solution (pCd = 3·0) containing 6·7 mM-$CdATP^{2-}$ and 1·1 mM-$MgATP^{2-}$. The force increased initially to about 80% of the maximum response due to a rapid increase in Cd^{2+} concentration and then it decreased to about 50% of the maximum response as the $CdATP^{2-}$ concentration gradually increased in the preparation. This result shows that $CdATP^{2-}$ has an inhibitory effect on the force response, presumably by competing with $MgATP^{2-}$ for the metal–nucleotide binding site on the myosin.

Force activation by Ni^{2+}

The activation solutions containing Ni^{2+} had a higher level of K^+ than those solutions containing Ba^{2+}, Ca^{2+}, Cd^{2+} and Sr^{2+}, because for the Ni^{2+} solutions we had to use the chloride salt. Nickel carbonate having a sufficiently high degree of purity was not available commercially.

The most important observation using Ni^{2+} solutions was that only a transient contractile response could be obtained when Ni^{2+} concentration in the solutions was increased from less than 10^{-12} M to between 10^{-6} and 10^{-5} M. Subsequent activation by Ca^{2+} (pCa 6 or pCa 5·24) always resulted in greatly diminished force responses compared with responses from controls. The irreversible inactivation process that followed exposure to Ni^{2+} was accompanied by a change in the appearance of the myofibrillar preparations in that they became opaque. It appears, therefore, that Ni^{2+} can activate contraction in the concentration range 10^{-6}–10^{-5} M, but that exposure to Ni^{2+} also leads to irreversible damage of the proteins of the contractile apparatus.

DISCUSSION

The experiments described here demonstrate that, in addition to Ca^{2+} and Sr^{2+}, Ba^{2+} and Cd^{2+} can also activate the contractile apparatus of amphibian skeletal muscle directly. Moreover, the maximum level of force activation that can be induced by Ba^{2+} and Cd^{2+} appears to be the same as that induced by Ca^{2+}. These findings are rather surprising considering that Ba^{2+}, a divalent alkaline earth metal ion, and Cd^{2+}, a divalent heavy metal ion have very different properties with respect to their ability to bind to troponin C and to activate actomyosin ATP-ase. For example, Cd^{2+} was found to have a high affinity for the Ca^{2+}–Mg^{2+} sites of troponin C (Fuchs, 1974; Hartshorne & Boucher, 1974; Forsen, Thulin & Lilja, 1979; Ellis, Strang & Potter,

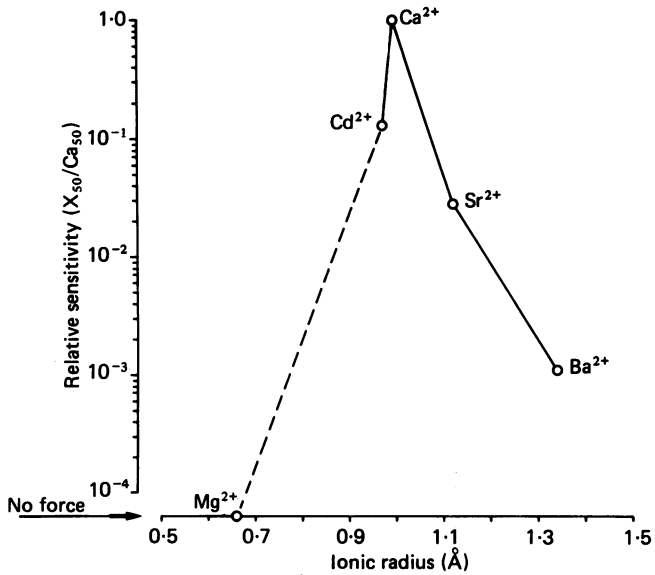

Fig. 6. Relative sensitivity (X_{50}/Ca_{50}) of the contractile mechanism of the frog skinned skeletal muscle fibre for Ca^{2+}, Cd^{2+}, Sr^{2+}, Ba^{2+} and Mg^{2+} as a function of the dehydrated ionic radius. X_{50}/Ca_{50} is defined as the ratio between the free concentration of the divalent ion X and Ca^{2+} at which half maximum isometric steady-state force was observed (data taken from Figs. 2*A* and 5*F*).

1984) and to activate the actomyosin ATP-ase to about 95% of the maximum Ca^{2+}-induced activation level (Hartshorne & Boucher, 1972). In contrast, Ba^{2+} was shown to have a very low affinity for troponin C (Ebashi & Endo, 1968; Fuchs, 1974; Hartshorne & Boucher, 1974) and it could not activate the actomyosin ATP-ase to more than about 40–50% of the maximal Ca^{2+}-induced activation level (Tonomura, 1973; Berson, 1974). It is also noteworthy that Ni^{2+}, a divalent heavy metal ion, for which no significant binding to troponin was demonstrated (Fischman & Swan, 1967; Fuchs, 1974; Hartshorne & Boucher, 1974; Winter, Head & Perry, 1974), did lead to a transient force development at relatively low concentrations (10^{-6}–10^{-5} M). This Ni^{2+} effect was, however, irreversible and therefore it was not studied in more detail.

A semilogarithmic plot of relative sensitivity (X_{50}/Ca_{50}) of the contractile apparatus to the various divalent ions, X, used in this study *versus* ionic radii is shown in Fig. 6. Notwithstanding the differences discussed above, this curve is similar to those obtained for the binding of divalent ions to tropinin C (Fuchs, 1974) and for myofibrillar ATP-ase activation (Tonomura, 1973), since it shows a peak corresponding to the radius of the Ca ion (0·99 Å). The curve in Fig. 6 indicates that the activation of the force controlling sites by divalent ions is mainly a function of the dehydrated ionic radius rather than of the specific chemical properties of the respective cations.

Our results obtained with Ba^{2+} and Cd^{2+} and Ni^{2+} are certainly important for the qualitative interpretation of contractile responses of intact (e.g. Heilbrunn & Wiercinski, 1947; Caldwell & Walster, 1963; Matsumura & Mashima, 1976; Potreau & Raymond, 1980) and skinned muscle preparations (Stephenson & Podolsky,

1977*a*, *b*) because they show that the contractile apparatus in amphibians can be at least partially activated by Cd^{2+} and Ba^{2+} concentrations as low as 1 and 10 μM respectively.

Furthermore, the results obtained with Ba^{2+} and Cd^{2+} are important for the better understanding of the mechanism of regulation of contraction. Both the Ba^{2+} and the Cd^{2+} force-activation curves (Figs. 2*A*, 3, 4 and 5*F*) are significantly flatter than those for Ca^{2+} and Sr^{2+} (Fig. 2*A*) indicating a lower degree of co-operativity in the process leading to force development for Ba^{2+} and Cd^{2+} than for Ca^{2+} and Sr^{2+}. This situation can arise, for example, if the specific sites involved in force regulation differ much more in their binding affinities for Ba^{2+} and Cd^{2+} than for Ca^{2+} and Sr^{2+}.

A set of reaction schemes which can explain all the steady-state results is shown below:

$$Ca^{2+} + R \overset{K_1^{Ca}}{\rightleftharpoons} CaR + Ca^{2+} \overset{K_2^{Ca}}{\rightleftharpoons} Ca_2R + Ca^{2+} \overset{K_3^{Ca}}{\rightleftharpoons} Ca_3R \begin{cases} + Ca^{2+} \overset{K_4^{Ca}}{\rightleftharpoons} Ca_4R, & (2) \\ + Ba^{2+} \overset{K_4^{CaBa}}{\rightleftharpoons} Ca_3BaR^*, & (3) \end{cases}$$

$$Ba^{2+} + R \overset{K_1^{Ba}}{\rightleftharpoons} BaR + Ba^{2+} \overset{K_2^{Ba}}{\rightleftharpoons} Ba_2R + Ba^{2+} \overset{K_3^{Ba}}{\rightleftharpoons} Ba_3R \begin{cases} + Ba^{2+} \overset{K_4^{Ba}}{\rightleftharpoons} Ba_4R, & (4) \\ + Ca^{2+} \overset{K_4^{BaCa}}{\rightleftharpoons} Ba_3CaR, & (5) \end{cases}$$

$$P_{CaBa} = ([Ca_4R] + [Ba_4R] + [Ba_3CaR])/R_{total}. \quad (6)$$

Here R is the regulatory functional unit exhibiting four Ca-binding sites which can also be occupied by Ba^{2+} in the indicated way. K_i^{Ca}, K_i^{Ba} ($i = 1, 2, 3$ and 4), K_4^{BaCa} and K_4^{CaBa} are the corresponding equilibrium constants, P_{CaBa} is the *relative* isometric force and R_{total} is the total concentration of the (regulatory) functional units. The reaction schemes (2) and (4) describe the pure Ca^{2+}- and Ba^{2+}-induced force development respectively. Reaction schemes (4) and (5) can be reduced to reaction scheme (1) if the first two steps of reaction (4) equilibrate rapidly and if $K_1^{Ba} \cdot K_2^{Ba} \gg K_3^{Ba} \cdot K_4^{Ba}$, i.e. if the equivalent affinity constant for the first two Ba^{2+} is much higher than that for the last two Ba^{2+}. Only with this latter assumption it is possible to generate a Hill coefficient of 2 or lower for the Ba^{2+} activation curve as seen experimentally in Figs. 2 and 3.

Reaction scheme (5) indicates the possibility that Ca^{2+} may replace Ba^{2+} to form a hybrid product of reaction containing both Ba^{2+} and Ca^{2+} which could lead to force development, while reaction scheme (3) shows that another hybrid product of reaction Ca_3BaR^* may not lead to force activation. In this case Ba^{2+} competes with Ca^{2+} to form with Ca_3R either the complex Ca_4R or the complex Ca_3BaR^*, of which only the former could lead to force activation. The existence of the two types of Ca–Ba hybrids must be assumed in order to explain the experimental observation that the submaximal force response at a given pCa is higher in the presence of Ba^{2+} if force is less than about 30 % and lower in the presence of Ba^{2+} if force is higher than about 60 % of the maximum activated response. It is suggested therefore, that a study of the Ca–Ba intermediates at molecular level could yield important information about the mechanism of force regulation.

The experimental points in Figs. 2 and 4 are fitted by curves derived from the eqns. (2)–(6) and using the values of parameters mentioned in the Figure legends and Appendix. It is apparent that predictions from such a model for force regulation can fit the experimental data reasonably well.

From the results presented in this study, it is expected that the Ca^{2+}–Mg^{2+} sites on troponin C are directly responsible for force activation. This is contrary to the general belief expressed by many biochemists in the field, who consider that only the Ca^{2+} specific sites on troponin are involved in regulation (see e.g. Ellis *et al.* 1984). Strong support for the involvement of the Ca^{2+}–Mg^{2+} sites in regulation is provided by the Cd^{2+} results which show that force is activated at Cd^{2+} levels (10^{-6}–10^{-5} M, Fig. 5) where Cd^{2+} can only bind to the Ca^{2+}–Mg^{2+} sites on troponin (Ellis *et al.* 1984). The amount of force generated at such low Cd^{2+} concentrations cannot be due to the small variation of $MgATP^{2-}$ and $CdATP^{2-}$ in solutions, particularly when it was found that force is inhibited rather than stimulated by $CdATP^{2-}$ (Fig. 5*E*). Also, separate experiments with mammalian fast-twitch muscle fibres and nitrilotriacetate (Moisescu, 1976; Ellis *et al.* 1984) as the main buffer for Cd^{2+} in solutions further support this view. Using the same affinity constants for the binding of the divalent ions to nitrilotriacetate as considered by Ellis *et al.* (1984) and similar ionic conditions to those described in this paper with respect to ATP, K^+, Na^+, Mg^{2+}, creatine phosphate, pH and ionic strength, we found that the skinned fast-twitch fibres of the rat (from the extensor digitorum longus muscle, Stephenson & Williams, 1981) are nearly maximally activated in the presence of 10^{-6} M-Cd^{2+}. According to the results of Ellis *et al.* (1984) only the Ca^{2+}–Mg^{2+} sites on troponin would be saturated with Cd^{2+} at this Cd^{2+} concentration, which is more than three orders of magnitude lower than that required for the Cd^{2+} saturation of the Ca^{2+}-specific sites on troponin. The possibility cannot be ruled out, however, that other force regulatory sites may also operate in the vertebrate muscle in addition to the Ca^{2+}–Mg^{2+} sites on troponin (see e.g. Moisescu, 1976; Stephenson & Williams, 1981). The fact that the characteristics of the Ba^{2+} and Cd^{2+} force activation curves are different from those of the Ca^{2+} and Sr^{2+} curves certainly warrants a more detailed comparative investigation of Ba^{2+}, Cd^{2+} and Ca^{2+} binding to troponin and to myofibrils, to elucidate where differences occur.

Finally, our observation that for given conditions, the process of force activation by Ba^{2+} is considerably slower than the activation by Ca^{2+}, can be used to improve the resolution of kinetic studies on the muscle regulatory systems.

APPENDIX

Derivation of the expression for P_{CaBa} from eqns. (2)–(6)

If $K_1^{Ca} \ll K_2^{Ca} \ll K_3^{Ca} \ll K_4^{Ca}$, $K_1^{Ba} \ll K_2^{Ba}$ and $K_3^{Ba} \ll K_4^{Ba}$ so that the concentrations of the intermediary products BaR, Ba_3R, CaR, Ca_2R and Ca_3R are always negligibly small compared to R_{total}, then from eqns. (2)–(6) it follows that:

$$\begin{aligned} P_{CaBa} = (&K_1^{Ba} . K_2^{Ba} . K_3^{Ba} . K_4^{Ba} . [Ba^{2+}]^4 + K_1^{Ca} . K_2^{Ca} . K_3^{Ca} . K_4^{Ca} . [Ca^{2+}]^4 \\ &+ K_1^{Ba} . K_2^{Ba} . K_3^{Ba} . K_4^{BaCa} . [Ba^{2+}]^3 . [Ca^{2+}]) \ (1 + K_1^{Ba} . K_2^{Ba} . [Ba^{2+}]^2 \\ &+ K_1^{Ba} . K_2^{Ba} . K_3^{Ba} . K_4^{Ba} . [Ba^{2+}]^4 + K_1^{Ba} . K_2^{Ba} . K_3^{Ba} . K_4^{BaCa} . [Ba^{2+}]^3 . [Ca^{2+}] \\ &+ K_1^{Ca} . K_2^{Ca} . K_3^{Ca} . K_4^{CaBa} . [Ca^{2+}]^3 . [Ba^{2+}] + K_1^{Ca} . K_2^{Ca} . K_3^{Ca} . K_4^{Ca} . [Ca^{2+}]^4)^{-1}, \end{aligned} \quad (A\ 1)$$

where P_{CaBa} is the relative isometric force when both ions are present.

In the absence of Ca^{2+}, eqn. (A 1) reduces to the expression:

$$P_{Ba} = K_1^{Ba} . K_2^{Ba} . K_3^{Ba} . K_4^{Ba} . [Ba^{2+}]^4 . (1 + K_1^{Ba} . K_2^{Ba} . [Ba^{2+}]^2 + K_1^{Ba} . K_2^{Ba} . K_3^{Ba} . K_4^{Ba} . [Ba^{2+}]^4)^{-1}. \quad (A\ 2)$$

Assuming further, that $K_1^{Ba} . K_2^{Ba} \gg K_3^{Ba} . K_4^{Ba}$, which is equivalent to $K_1^{Ba} . K_2^{Ba} . [Ba^{2+}]^2 \gg 1$ at subthreshold $[Ba^{2+}]$ ($P_{Ba} < 0{\cdot}01$), it follows that for the range of interest in Figs. 2 and 3, the equation (A 2) reduces to:

$$P_{Ba} = K_3^{Ba} . K_4^{Ba} . [Ba^{2+}]^2 / (1 + K_3^{Ba} . K_4^{Ba} . [Ba^{2+}]^2), \quad (A\ 3)$$

where $K_3^{Ba} = k_1'/k_{-1}'$ and $K_4^{Ba} = k_2'/k_{-2}'$ (see eqn. (1)).

This is a typical Hill equation for Ba^{2+} with $n = 2$. In the absence of Ba^{2+}, the equation (A 1) becomes

$$P_{Ca} = K_1^{Ca} . K_2^{Ca} . K_3^{Ca} . K_4^{Ca} . [Ca^{2+}]^4 / (1 + K_1^{Ca} . K_2^{Ca} . K_3^{Ca} . K_4^{Ca} . [Ca^{2+}]^4), \quad (A\ 4)$$

which is a typical Hill equation for Ca^{2+} with $n = 4$.

At a constant subthreshold Ba^{2+} concentration ($K_1^{Ba} . K_2^{Ba} . [Ba^{2+}]^2 \gg 1$; $K_3^{Ba} . K_4^{Ba} . [Ba^{2+}]^2 < 0{\cdot}01$), the expression for P_{CaBa}, is approximated by:

$$P_{CaBa} = (A . [Ca^{2+}]^4 + C . [Ca^{2+}]) / (1 + A . [Ca^{2+}]^4 + B . [Ca^{2+}]^3 + C . [Ca^{2+}]), \quad (A\ 5)$$

where $A = K_1^{Ca} . K_2^{Ca} . K_3^{Ca} . K_4^{Ca} / (K_1^{Ba} . K_2^{Ba} . [Ba^{2+}]^2)$,

$B = K_1^{Ca} . K_2^{Ca} . K_3^{Ca} . K_4^{CaBa} / (K_1^{Ba} . K_2^{Ba} . [Ba^{2+}])$, and

$C = K_3^{Ba} . K_4^{BaCa} . [Ba^{2+}]$.

We are grateful to Professor H. Ch. Lüttgau for his continuous interest and encouragement during this work and thank Dr A. Wright for critically reading the manuscript. The financial support of the Friedrich-Ebert-Stiftung (R.T.) and ARGS (D.G.S.) is gratefully acknowledged.

REFERENCES

ALMERS, W. & PALADE, P. T. (1981). Slow calcium and potassium currents across frog muscle membrane: measurements with a vaseline-gap technique. *Journal of Physiology* **312**, 159–176.

ASHLEY, C. C. & MOISESCU, D. G. (1977). Effect of changing the composition of the bathing solutions upon the isometric tension–pCa relationship in bundles of crustacean myofibrils. *Journal of Physiology* **270**, 627–652.

BERSON, G. (1974). Ca^{2+}, Sr^{2+}, and Ba^{2+} sensitivity of tropomyosin–troponin complex from cardiac and fast skeletal muscles. In *Calcium Binding Proteins*, ed. DRABIKOWSKI, W., STRZELECKA-GOLASZEWSKA, H. & CARAFOLI, E., pp. 197–201. Amsterdam: Elsevier.

BLINKS, J. R., MATTINGLY, P. H., JEWELL, B. R., VAN LEEUWEN, M., HARRER, G. C. & ALLEN, D. G. (1978). Practical aspects of the use of aequorin as a calcium indicator: assay, preparation, microinjection, and interpretation of signals. In *Methods in Enzymology*, vol. 57, ed. DE LUCA, M. A., pp. 292–328. New York: Academic Press.

CALDWELL, P. C. & WALSTER, G. E. (1963). Studies on the micro-injection of various substances into crab muscle fibres. *Journal of Physiology* **169**, 353–372.

CAPUTO, C. (1981). Nickel substitution for calcium and the time course of potassium contractures of single muscle fibres. *Journal of Muscle Research and Cell Motility* **2**, 167–182.

DONALDSON, S. K. B. & KERRICK, W. G. L. (1975). Characterization of the effects of Mg^{2+} on Ca^{2+}- and Sr^{2+}-activated tension generation of skinned skeletal muscle fibers. *Journal of General Physiology* **66**, 427–444.

EBASHI, S. & ENDO, M. (1968). Calcium ion and muscle contraction. *Progress in Biophysics and Molecular Biology* **18**, 123–183.

ELLIS, P. D., STRANG, P. & POTTER, J. D. (1984). Cadmium-substituted skeletal troponin C. Cadmium-113 NMR spectroscopy and metal binding investigations. *Journal of Biological Chemistry* **259**, 10348–10356.

FISCHMAN, D. A. & SWAN, R. C. (1967). Nickel substitution for calcium in excitation–contraction coupling of skeletal muscle. Divalent cations in E–C coupling. *Journal of General Physiology* **50**, 1709–1728.

FORSEN, S., THULIN, E. & LILJA, H. (1979). ^{113}Cd NMR in the study of calcium binding proteins: troponin C. *FEBS Letters* **104**, 123–126.

FRANK, G. B. & ROHANI, F. (1982). Ba^{2+} ions block K^+-induced contractures by antagonizing K^+-induced membrane depolarization in frog skeletal muscle fibres. *Canadian Journal of Physiology and Pharmacology* **60**, 47–51.

FUCHS, F. (1974). Chemical properties of the calcium receptor site of troponin as determined from binding studies. In *Calcium Binding Proteins*, ed. DRABIKOWSKI, W., STRZELECKA-GOLASZEWSKA, H. & CARAFOLI, E., pp. 1–27. Amsterdam: Elsevier.

HARTSHORNE, D. J. & BOUCHER, L. J. (1972). Calcium and the control of muscle activity. In *Hibernation and Hypothermia: Perspectives and Challenges*, ed. SOUTH, F. E., HANNON, J. P., WILLIS, J. R., PENGELLEY, E. T. & ALPERT, N. R., pp. 357–371. Amsterdam: Elsevier.

HARTSHORNE, D. J. & BOUCHER, L. J. (1974). Ion binding by troponin. In *Calcium Binding Proteins*, ed. DRABIKOWSKI, W., STRZELECKA-GOLASZEWSKA, H. & CARAFOLI, E., pp. 29–49. Amsterdam: Elsevier.

HEILBRUNN, L. V. & WIERCINSKI, F. J. (1947). The action of various cations on muscle protoplasm. *Journal of Cellular and Comparative Physiology* **29**, 15–29.

JULIAN, F. J. (1971). The effect of calcium ion on the force–velocity relation of briefly glycerinated frog muscle fibres. *Journal of Physiology* **218**, 117–145.

MATSUMURA, M. & MASHIMA, H. (1976). Contraction produced by intracellular injection of calcium, strontium and barium in the single crayfish muscle fibers. *Japanese Journal of Physiology* **26**, 145–157.

MOISESCU, D. G. (1976). Kinetics of reaction in calcium-activated skinned muscle fibres. *Nature* **262**, 610–613.

MOISESCU, D. G. & THIELECZEK, R. (1978). Calcium and strontium concentration changes within skinned muscle preparations following a change in the external bathing solution. *Journal of Physiology* **275**, 241–262.

MOISESCU, D. G. & THIELECZEK, R. (1979). Sarcomere length effects on the Sr^{2+} and Ca^{2+} activation curves in skinned frog muscle fibres. *Biochimica et biophysica acta* **546**, 64–76.

POTREAU, D. & RAYMOND, G. (1980). Slow inward barium current and contraction on frog single muscle fibres. *Journal of Physiology* **303**, 91–109.

SAKS, V. A., ROSENSTRAUKH, L. V., SMIRNOV, V. N. & CHAZOV, E. I. (1978). Role of creatine-phosphokinase in cellular function and metabolism. *Canadian Journal of Physiology and Pharmacology* **56**, 691–706.

SILLÉN, L. G. & MARTELL, A. E. (1964). *Stability Constants of Metal–Ion Complexes*. Special Publication No. **17**. London: The Chemical Society.

SILLÉN, L. G. & MARTELL, A. E. (1970). *Stability Constants of Metal–Ion Complexes. Supplement 1*. Special Publication No. **25**. London: The Chemical Society.

STEPHENSON, D. G. & WILLIAMS, D. A. (1980). Activation of skinned arthropod muscle fibres by Ca^{2+} and Sr^{2+}. *Journal of Muscle Research and Cell Motility* **1**, 73–87.

STEPHENSON, D. G. & WILLIAMS, D. A. (1981). Calcium-activated force responses in fast- and slow-twitch skinned muscle fibres of the rat at different temperatures. *Journal of Physiology* **317**, 281–302.

STEPHENSON, D. G. & WILLIAMS, D. A. (1982). Effects of sarcomere length on the force–pCa relation in fast- and slow-twitch skinned muscle fibres from the rat. *Journal of Physiology* **333**, 637–653.

STEPHENSON, E. W. & PODOLSKY, R. J. (1977*a*). Regulation by magnesium of intracellular calcium movement in skinned muscle fibers. *Journal of General Physiology* **69**, 1–16.

STEPHENSON, E. W. & PODOLSKY, R. J. (1977*b*). Influence of magnesium on chloride-induced calcium release in skinned muscle fibres. *Journal of General Physiology* **69**, 17–35.

THIELECZEK, R. (1982). Untersuchungen an der enthäuteten Skelettmuskelfaser des Frosches zur Aktivierbarkeit des kontraktilen Systems und zur Ca^{2+}-Freisetzung und -Aufnahme des Sarcoplasmatischen Reticulums. Ph.D. Thesis. Ruhr University, Bochum.

TONOMURA, Y. (1973). *Muscle Proteins, Muscle Contraction and Cation Transport.* Baltimore: University Park Press.

WALLIMAN, T., TURNER, D. C. & EPPENBERGER, H. M. (1977). Localization of creatine kinase isoenzymes in myofibrils. I. Chicken skeletal muscle. *Journal of Cell Biology* **75**, 297–317.

WINTER, M. R. C., HEAD, J. F. & PERRY, S. V. (1974). Conformational changes and complex formation by troponin C. In *Calcium Binding Proteins*, ed. DRABIKOWSKI, W., STRZELECKA-GOLASZEWSKA, H. & CARAFOLI, E., pp. 109–127. Amsterdam: Elsevier.